Vol. 44, No. 2 (2022) 199-211, DOI: 10.24874/ti.1075.03.21.05

Tribology in Industry

www.tribology.rs

RESEARCH

Comparative Investigations on Microstructure and Slurry Abrasive Wear Resistance of NiCrBSi and NiCrBSi-WC Composite Hardfacings Deposited on 304 Stainless Steel

Vivek D. Kalyankar[a], Sachin P. Wanare[a,*]

[a]*Mechanical Engineering Department, S. V. National Institute of Technology, Surat, India.*

Keywords:

Slurry abrasive wear resistance
NiCrBSi
NiCrBSi-WC
Microstructure
Plasma transferred arc welding
AISI 304 stainless steel

* Corresponding author:

Sachin P. Wanare
E-mail: spwanare@gmail.com

Received: 16 March 2021
Revised: 4 May 2021
Accepted: 31 May 2021

A B S T R A C T

The aim of this article is to minimize the premature failure of slurry pipelines caused due to slurry abrasive wear by depositing NiCrBSi and NiCrBSi-WC composite hardfacings on 304 stainless steel using plasma transferred arc welding and recommending the best combination after its comparison. Comparative analysis revealed that, the slurry abrasive wear resistance of NiCrBSi-WC composite hardfacing is 2.5 times better than that of NiCrBSi hardfacing and forty times than that of 304 stainless steel which is mainly due to the presence of WC and W2C phases along with chromium carbides and chromium borides. The typical microstructure of the NiCrBSi-WC hardfacing identified through scanning electron microscopy with energy dispersive spectroscopy consists of Ni-solid solution, blocky and needle shaped precipitates along with interdendritic eutectic precipitation and WC reinforcing particles are well dispersed in the nickel matrix. The worn-out morphology of NiCrBSi-WC composite hardfacing shows comparatively shallower grooves caused due to ploughing action which results in lower weight loss than NiCrBSi hardfacing and 304 stainless steel. The outcomes of comparative analysis in terms of significant improvement in slurry abrasive wear resistance of NiCrBSi-WC composite hardfacing may be beneficial to improve the service-life of slurry pipelines.

1. INTRODUCTION

Hydraulic transportation systems used in mineral processing industries are becoming popular due to their lower cost and less environmental impact [1,2]. In the mining industries, failure of several engineering components due to poor wear resistance is the universally faced problem [3]. The efficient tribological solutions in the mining industries may lead to a significant reduction in the expenses such as 40% of the friction losses, 26% of the workforce, 27% of the replacement of deteriorated parts and 7% of the production

losses [4,5]. The abrasive wear accounts about 50% of all wear problems in mining industries [6]. The slurry pipelines often fail due to their poor abrasive wear resistance which is mainly caused due to the flow of hard particles suspended in water over the component surface [1,2,7-9].

AISI 304 austenitic stainless steel (ASS) is widely used material for slurry pipelines of hydraulic transport systems due to its satisfactory mechanical properties and superior corrosion resistance [2,10,11]. However, it has poor wear resistance and hardness which leads to its premature failure in such an aggressive wear conditions [12,13]. Surface modification techniques are widely adopted to enhance its wear resistance and hardness by the deposition of a highly wear resistant layer on the surface.

Weld overlay processes are widely used for the deposition of thick hardfacings on the component surface working in aggressive working environments in order to increase their service life [14,15]. Amongst various weld overlay processes, plasma transferred arc welding (PTAW) is being widely adopted for deposition of wear resistant coatings including metal matrix composite (MMC) coatings due to its numerous benefits such as lower operation cost, higher deposition efficiency, good metallurgical bonding, lower dilution rates, complete automation, minimum thermal distortion, concentrated heat input, precision in controlling process parameters, excellent arc stability, consistency in results, etc. [16-21]. Because of these benefits, PTAW can effectively achieve superior properties of overlay materials by appropriate control on process parameters.

Nickel-based hardfacing materials are widely used for the protection of several engineering components from severe corrosive and wear conditions in industrial sectors such as power, mineral and oil industries [21,23-25]. Nickel-based hardfacing materials are widely used as MMC's due to their high toughness for the applications where high wear resistant properties are required [26]. MMC's are becoming popular which consist of hard and brittle carbides embedded in metal binders [20,27]. The carbides and matrix present in MMC's performs an interface reaction which binds the carbides with the matrix to form an interface which is responsible for the mechanical behavior of the hardfacing [28]. The addition of ceramic particles in nickel-based alloys significantly improves the mechanical properties. Fine dispersion of ceramic particles in the matrix will act as a breakpoint to the crack propagation. MMC's can sustain higher compressive as well as tensile stresses, which is possible by transferring the applied load from the ductile matrix to the reinforcement phases [29]. The abrasive wear resistance of the metallic matrix can be significantly enhanced by the addition of tungsten carbide (WC) [14,30]. The NiCrBSi alloys have low melting point about 1025 °C which allows WC reinforcing particles to undergo the deposition process without degradation as compared to Fe based hardfacing alloys [31]. Nickel matrix has higher toughness and WC has high hardness (~2600 HV). Hence, the combination of these alloys provides excellent wear resistance [30]. Maslarevic et al. [20] have performed investigations on microstructure and erosive wear resistance of WC/NiBSi and WC/NiCrBSi MMC coatings deposited by PTAW and flame spray process respectively. It is revealed that the WC/NiBSi coating shows superior hardness and wear resistance which is mainly attributed to the composition and morphology of the coating material along with capability of PTAW process for the production of WC reinforced MMC coatings with significantly lower amount of porosity. Investigations performed by Deenadayalan and Murali [21] on dry sliding wear behaviour of NiCrBSi and NiCrBSi-WC composite hardfacings deposited on 316L stainless steel by PTAW revealed that the NiCrBSi-WC shows significant improvement in sliding wear resistance.

In this work, two approaches have been considered to ensure the deposition of hardfacings with improved microhardness and slurry abrasive wear resistance along with desired microstructural characteristics and good metallurgical bond with the substrate material. The first approach consists of the deposition of NiCrBSi hardfacing without addition of WC reinforcing particles (NiCrBSi) and the second approach consist of the deposition of NiCrBSi hardfacing with addition of 20 weight % of WC reinforcing particles (NiCrBSi-WC). AISI 304 ASS is considered as the substrate material and PTAW process is

adopted for the deposition of hardfacings in case of both the approaches for fair comparison purpose. The main objective is to bring about the thorough comparative investigations on the microstructure, microhardness, slurry abrasive wear behavior and worn-out morphology of NiCrBSi and NiCrBSi-WC composite hardfacings which may be beneficial to improve the service life of slurry pipelines used in mineral processing industries.

2. MATERIALS AND METHODS

2.1 Description of materials

AISI 304 ASS of size 200 mm x 100 mm x 12 mm was used as the substrate material. Nickel-based hardfacing powder NiCrBSi of size 45 to 180 µm from Wall Colmonoy Ltd. and WC reinforcing powder of size 45 to 150 µm from Hoganas, Co. Ltd. was used for deposition of hardfacings. The chemical composition of substrate and hardfacing materials is presented in Table 1.

Table 1. Chemical composition in (wt. %) of substrate and hardfacing materials.

Element	Chemical composition [%]								
	Cr	C	Fe	B	Si	Mn	P	Ni	W
304 ASS (Substrate)	19.92	0.04	Bal.	---	0.37	1.52	0.03	8.11	---
NiCrBSi Hardfacing	6.64	0.6	4.54	3.02	4.52	---	---	Bal.	---
WC Hardfacing	---	3-6	---	---	---	---	---	---	Bal.

2.2 PTAW process parameters

Multi-track experiments having 50% width overlap as shown in Fig. 1 were performed by PTAW to achieve crack-free deposition of NiCrBSi and NiCrBSi-WC composite hardfacings as per the process parameters presented in Table 2.

Table 2. PTAW process parameters for multi-track experiments.

Samples	Transferred arc current (A)	Powder feed rate (g/min)	Travel speed (mm/min)	Stand-off distance (mm)
NiCrBSi	120	16	55	8
NiCrBSi-WC	120	16	55	8

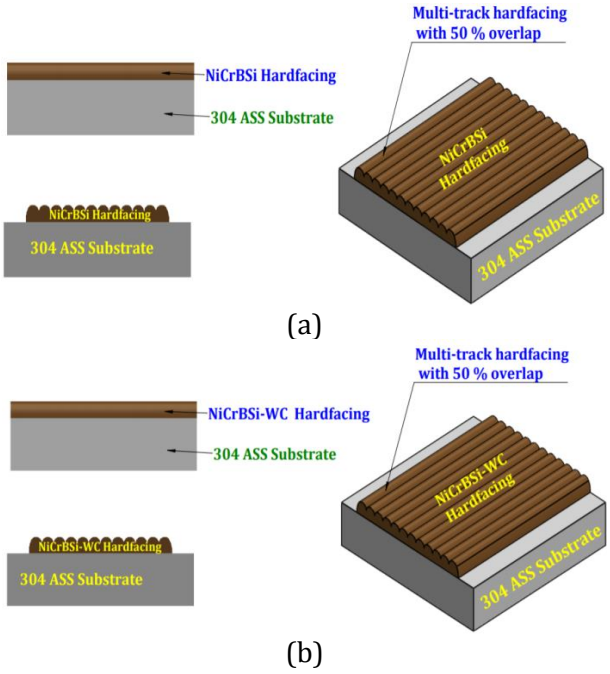

Fig. 1. Schematic diagram of multi-track hardfacing with 50 % overlap for (a) NiCrBSi sample and (b) NiCrBSi-WC sample.

2.3 Hardfacing preparation

The hardfacing powders were heated to 100°C in order to remove moisture present if any and to increase its flowability. From the trial experiments, it was observed that the addition of WC beyond 20% lead to formation of cracks perpendicular to hardfacing with poor metallurgical bond between substrate and hardfacing. Hence, in order to achieve crack-free deposition, multi-track experiments were performed with and without addition of 20 weight % of WC reinforcing particles to NiCrBSi hardfacing. The WC reinforcing particles were homogeneously mixed with NiCrBSi hardfacing powder with the help of planetary ball mill for 2 hours and mixed powders had been directly poured in PTAW hopper without storing so as to avoid the settling of higher density WC particles [14]. It is observed that the deposition of NiCrBSi hardfacing with and without addition of WC reinforcing particles lead to the formation of cracks perpendicular to the welding direction if preheating is not performed to substrate material 304 ASS. Hence, preheating and interpass temperature at 350 to 400°C was maintained during the deposition of hardfacings in order to avoid the heat affected zone cracking [32,33]. The plasma gas flow rate, shielding gas flow rate and carrier gas flow rate were kept constant as 2

litre/min, 7 litre/min and 10 litre/min respectively. The PTAW parameters were tuned to obtain approximately 3 mm thickness of hardfacings. The surfaces of the hardfacings were ground by using a surface grinder to maintain uniform thickness of 2 mm. Pure argon was used as shielding gas, carrier gas and plasma gas. After successful completion of multi-track layers, the test coupons were subjected to sand cooling to avoid formation of cracks and to relieve internal stresses. The hardfaced samples were subjected to dye penetrant test for examination of any surface defects [34].

2.4 Microstructural characterization

Samples for microstructural examination of NiCrBSi and NiCrBSi-WC composite hardfacings were prepared as per the standard metallographic procedure. Etching of metallographic samples was performed with a solution of HNO_3 and HCl (1:4) for etching time of 60 seconds [35,36]. Microstructural characterization was examined by field emission scanning electron microscopy (FESEM). FESEM equipped with energy dispersive spectroscopy (EDS) is capable of determining the elemental composition of the hardfacings in order to identify the changes in the mechanical properties of the hardfacings. The semiquantitative chemical analysis for the elements such as W, Cr, Ni, Fe, C, Si and B was performed by area scan and spot analysis using EDS under accelerating voltage of 20 keV [37]. The XRD spectra were taken by X-ray diffractometer (XRD) with Cu Kα radiation for scanning rate of 2°/min and range of 0 to 80° (2θ). The Fe dilution measurement was carried out using SEM-EDS considering the percentage of Fe present in the deposited hardfacing, substrate and hardfacing powder according to equation 1 [15].

$$\text{Fe dilution}(\%) = \frac{\text{Fe}(\%)\,\text{hardfacing} - \text{Fe}(\%)\,\text{powder}}{\text{Fe}(\%)\,\text{substrate} - \text{Fe}(\%)\,\text{powder}} \times 100 \quad (1)$$

2.5 Microhardness and slurry abrasive wear test

Microhardness of multi-track specimens was measured across the cross section of each hardfaced specimen with Vicker's microhardness tester for load of 500 grams and dwell time of 10 seconds. Indentations were taken at the interval of 300 μm from the interface. The wet sand and rubber wheel slurry abrasive wear test as per the schematic shown in Fig. 2 with 50/70 μm size quartz sand as abradant was used for performance of wear test. The high precision weighing machine was used for weighing the test specimens before and at the end of each test to find out the weight loss. The test specimens were extracted from multi-track hardfacings and substrate material each in rectangular shape with standard dimensions of 25.4 +/- 0.8 mm (width), 57.2 +/- 0.8 mm (length) and 14 mm (thickness). As per ASTM G105, following parameters were selected: load-222N, speed-245 rpm, test durations-1000 revolutions of wheel and wear test was repeated for 50, 60 and 70 durometer hardness wheels as per standard procedure. The abrasive slurry was consisted of a mixture of 0.940 kg of deionized water and 1.5 kg of a rounded grain quartz sand as specified by American Foundry Society. Weight loss was obtained by the least square line method as per ASTM G105 standard. The test results were reported in terms of weight loss of hardfacings and compared with substrate material. Worn-out surface analysis for hardfaced specimens and substrate material was performed by FESEM to understand the wear mechanism.

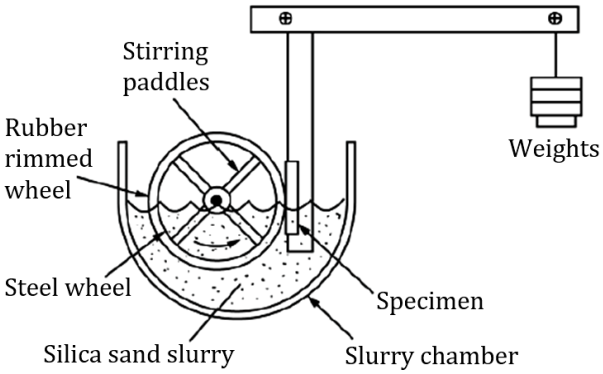

Fig. 2. Schematic of slurry abrasion wear testing apparatus [11,38].

3. RESULTS AND DISCUSSIONS

3.1 Microstructural analysis

Fig. 3 shows XRD spectra for NiCrBSi hardfacing and NiCrBSi-WC composite hardfacing. The chemical composition of hardfacing materials showed significant impact on the presence of numerous phases. The NiCrBSi hardfacing shows X-ray diffraction pattern corresponding to γ-Ni, $Cr_{23}C_6$, Cr_7C_3, CrB, Ni_3B, $FeNi_3$ and Fe_2Si phases as

examined from the analysis and comparison [25,39]. It is reported that the microhardness of NiCrBSi alloy is largely varied by the type and amounts of hard precipitates, such as chromium borides and chromium carbides [40]. The NiCrBSi-WC composite hardfacing shows X-ray diffraction pattern corresponding to γ-Ni, $Cr_{23}C_6$, Cr_7C_3, CrB, Ni_3B, $FeNi_3$, Fe_2Si, WC and W_2C phases as examined from the analysis and comparison [25,39].

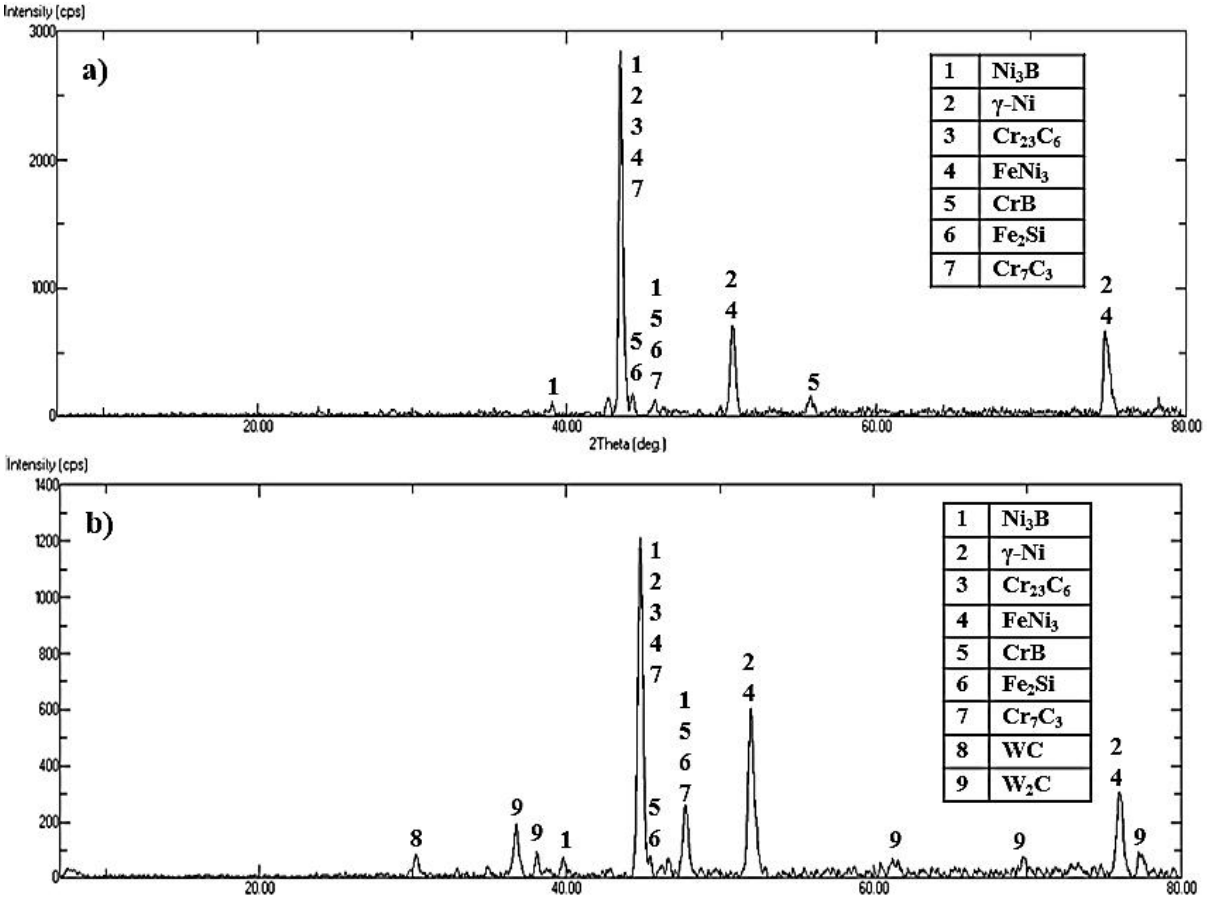

Fig. 3. XRD patterns of as deposited hardfacings for a) NiCrBSi sample and b) NiCrBSi-WC sample.

The FESEM-EDS area scan analysis for NiCrBSi hardfacing and NiCrBSi-WC composite hardfacing was performed in order to analyse the percentage of Fe diluted from the substrate, as shown in Fig. 4 and Fig. 5 respectively. It is revealed that NiCrBSi hardfacing contains 23.3 % Fe and NiCrBSi-WC composite hardfacing contains 20.6 % Fe. The measurement of Fe dilution for NiCrBSi and NiCrBSi-WC composite hardfacing is calculated as per equation 1 as 28.66 % and 24.54 % respectively. It is the well-established fact that the increase in Fe dilution significantly deteriorates the hardness and wear resistance of the hardfacings [41]. The lower Fe dilution in case of NiCrBSi-WC hardfacing is beneficial for higher volume fraction of hard phases as discussed in further analysis.

Fig. 6 shows cross-sectional micrographs obtained by FESEM for NiCrBSi hardfacing. It is clearly seen from Fig. 6a that the NiCrBSi hardfacing has a good metallurgical bond with the substrate material and the hardfacing is free of cracks. The microstructure of NiCrBSi hardfacing consists of interdendritic eutectic precipitations, needle shaped precipitates and nickel solid solution as seen in Fig. 6b. The elemental distribution obtained by FESEM-EDS spot analysis is shown in Fig. 6c and 6d and presented in Table 3 confirmed the presence of γ-Ni (nickel solid solution), chromium borides and chromium carbides. The presence of chromium carbides and chromium borides is attributed to the fact that the chromium has high affinity towards carbon and boron than that of nickel and iron, hence chromium and boron forms chromium borides and chromium and carbon forms chromium carbides [42]. Needle shaped chromium borides are mainly observed in the coating area which are responsible for higher slurry abrasive wear resistance as compared to the substrate material.

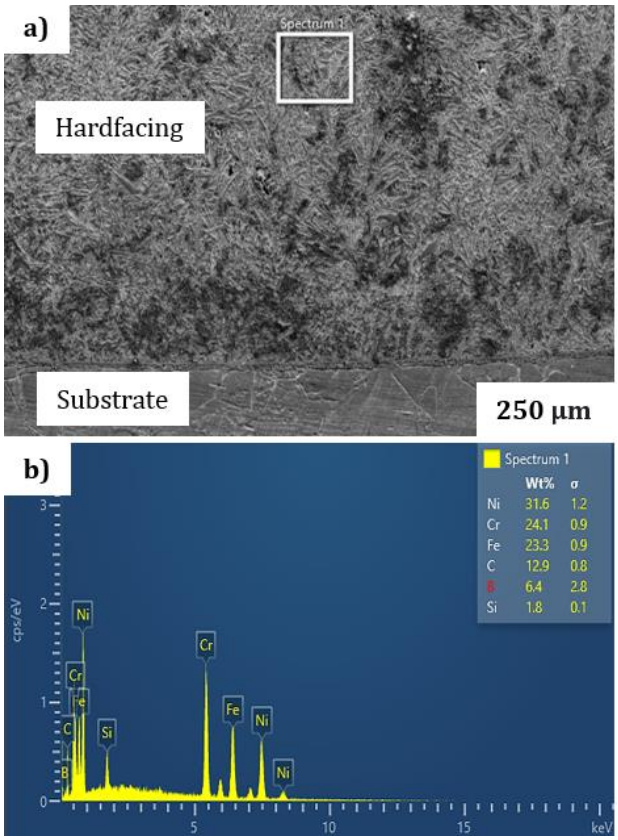

Fig. 4. a) and b) FESEM-EDS area scan analysis for NiCrBSi hardfacing.

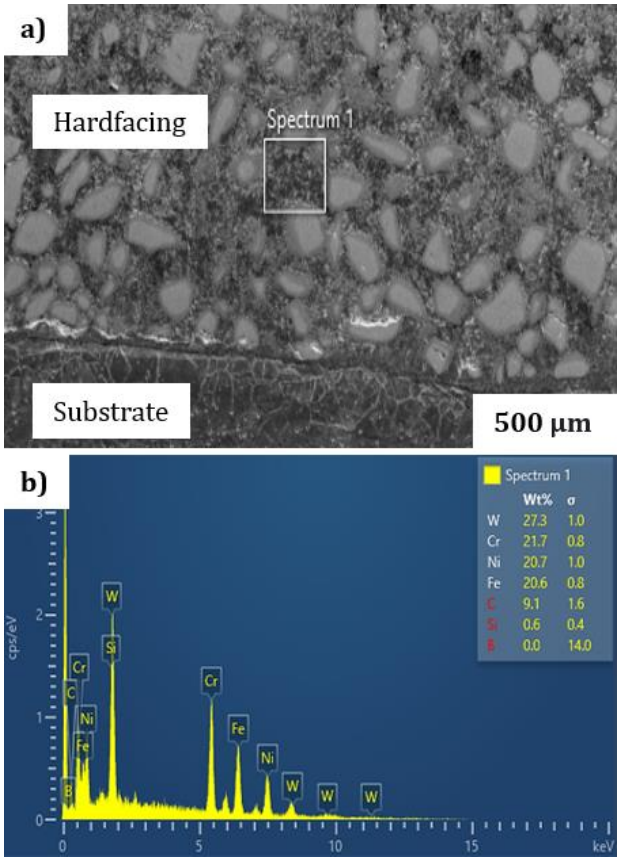

Fig. 5. a) and b) FESEM-EDS area scan analysis for NiCrBSi-WC hardfacing.

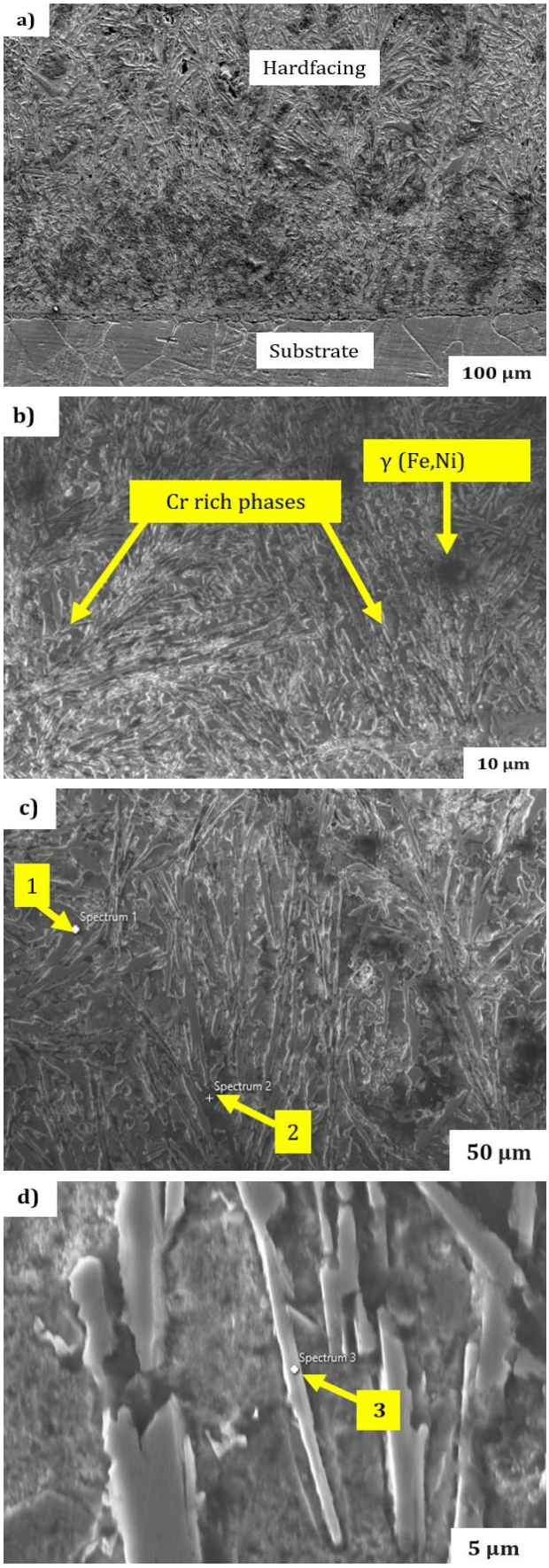

Fig. 6. a) and b) FEGSEM micrographs for microstructural examination of NiCrBSi hardfacing and c) and d) FESEM-EDS spot analysis.

Table 3. FESEM-EDS spot analysis of phases present in NiCrBSi hardfacing.

Elements (wt-%)	Ni	Cr	C	Fe	B	Si
Point 1	6.7	56.8	3.2	27.9	5.5	0.0
Point 2	50.9	10.0	7.7	25.8	2.7	2.9
Point 3	6.8	51.8	5.7	23.8	11.5	0.3

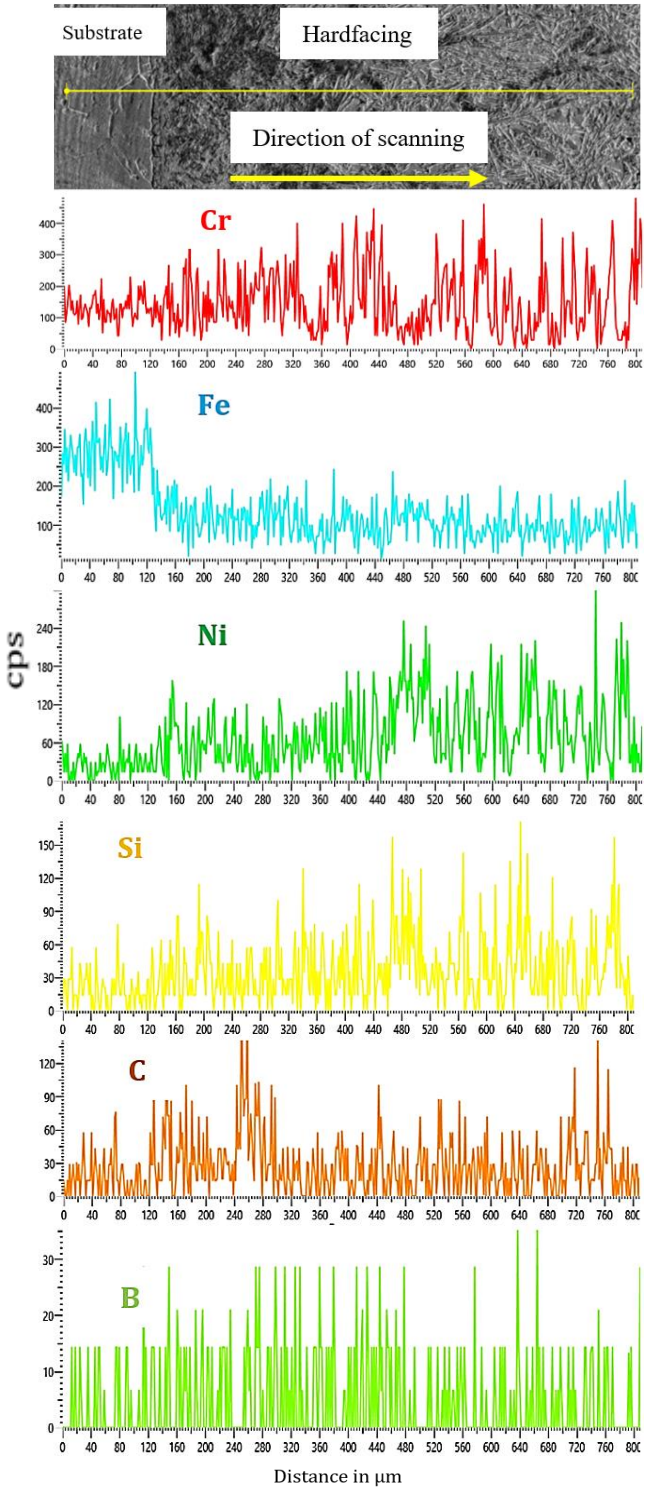

Fig. 7. FESEM EDS line scan analysis for NiCrBSi hardfacing.

As per the FESEM EDS line scan analysis for NiCrBSi hardfacing presented in Fig. 7, it is revealed that the Cr, Fe, Ni and other elements have significant change in the chemical composition from substrate towards the hardfacing region. It is clearly seen that the elements from substrate and hardfacing are diffused strongly from each other due to the high energy density heat source of plasma arc and formed good metallurgical bond.

Fig. 8 shows cross-sectional micrographs obtained by FESEM for NiCrBSi-WC composite hardfacing. It is clearly seen from Fig. 8a that the NiCrBSi-WC hardfacing has a good metallurgical bond with the substrate material. In particular, the hardfacing consists of dendritic nickel solid solution, blocky and needle shaped precipitates with interdendritic eutectic precipitation and WC reinforcing particles are well dispersed in the nickel matrix as seen in Fig. 8a and 8b. The WC reinforcing particles are appeared as densely packed at some locations near the interface between substrate and hardfacing, which may be attributed to higher density and higher melting point of WC as compared to the NiCrBSi hardfacing. It is observed that the selection of appropriate process parameters is crucial, particularly transferred arc current which is mainly responsible for heat input in order to avoid the dissolution of WC particles. In the present study, the dissolution of WC reinforcing particles is significantly controlled while depositing NiCrBSi-WC composite hardfacing by selecting appropriate process parameters. Above the interface, some microcracks are seen which may be attributed to higher differences between the melting points of WC and nickel matrix as well as high hardness of WC phases. The elemental distribution obtained by FESEM-EDS spot analysis as shown in Fig. 8c and 8d and presented in Table 4 confirmed the presence of tungsten carbides, chromium borides and chromium carbides phases along with nickel solid solution. The significant improvement in slurry abrasive wear performance of WC reinforced NiCrBSi hardfacing is mainly attributed to the presence of hard phases such as tungsten carbides, chromium carbides and chromium borides.

Table 4. FESEM-EDS spot analysis of phases present in NiCrBSi hardfacing.

Elements (wt-%)	W	Ni	Cr	C	Fe	B	Si
Point 1	93.7	0.1	0.0	6.0	0.2	0.0	0.0
Point 2	4.6	17.7	15.6	15.0	27.8	0.0	19.5
Point 3	7.9	5.8	43.7	10.9	29.7	1.3	0.7
Point 4	13.0	3.4	42.1	14.6	22.7	4.3	0.0

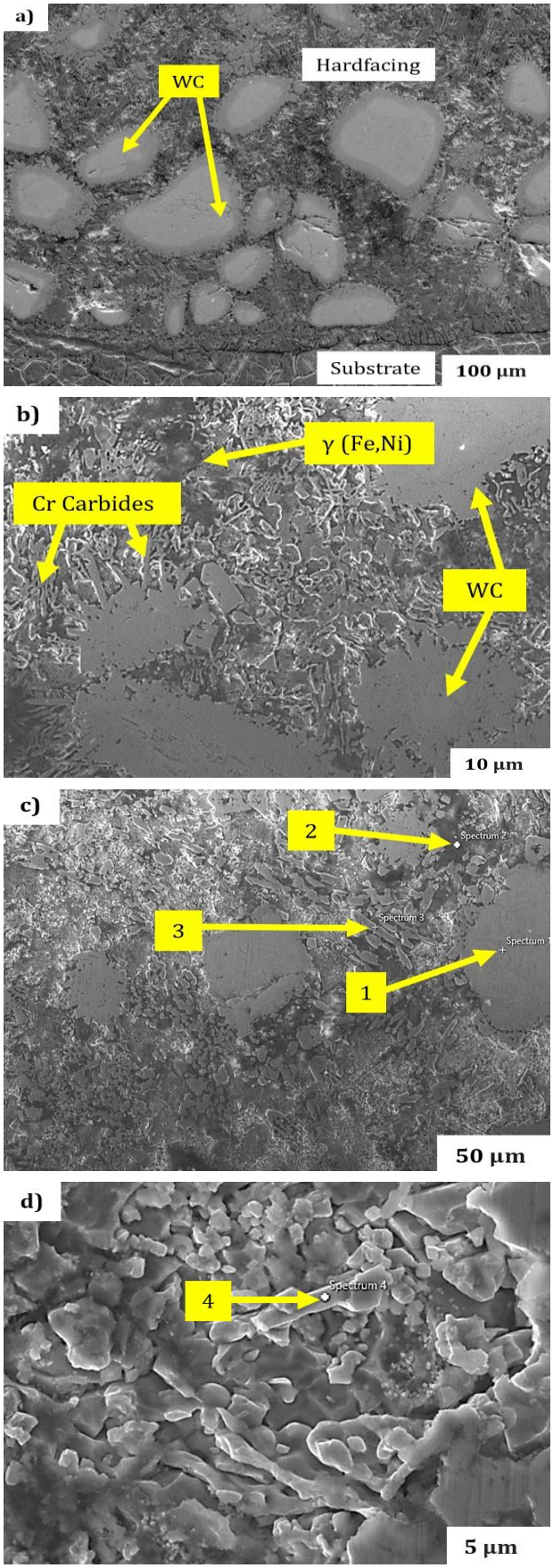

Fig. 8. a) and b) FEGSEM images for microstructure and c) and d) FESEM-EDS spot analysis of NiCrBSi-WC composite hardfacing.

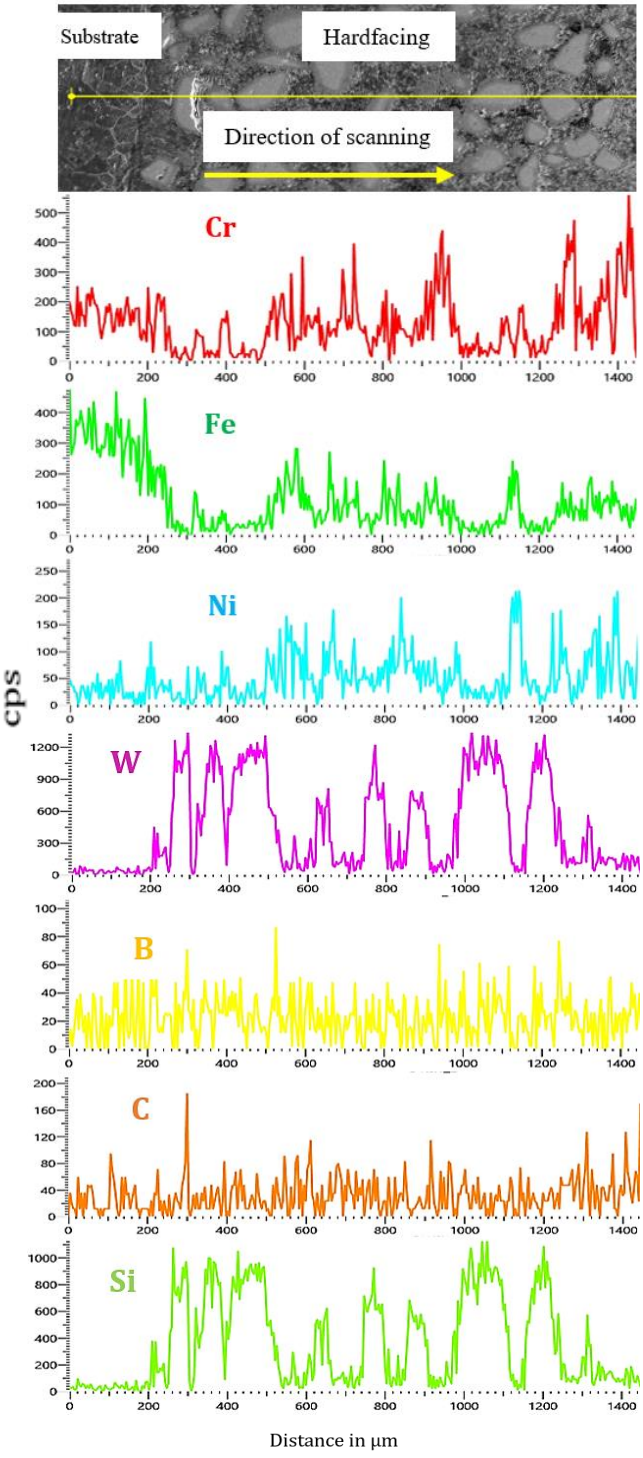

Fig. 9. FESEM EDS line scan analysis for NiCrBSi-WC hardfacing.

As per the FESEM EDS line scan analysis for NiCrBSi-WC hardfacing presented in Fig. 9, the Cr, Fe, W, Ni and other elements have significant change in chemical composition. Strong diffusion of elements of substrate and hardfacing from each other due to high heat energy from plasma arc confirmed the good metallurgical bond.

3.2 Microhardness analysis

Fig. 10 shows microhardness distribution across the cross section of as deposited NiCrBSi and NiCrBSi-WC composite hardfacing. The average microhardness of the substrate region is observed as 207 HV. The microhardness in the hardfacing region increases towards the top of the hardfacing region. The average microhardness of NiCrBSi and NiCrBSi-WC hardfacings are observed as 405 HV and 522 HV respectively. It is observed that, near the interface the percentage of Fe diluted from substrate material is comparatively higher which is responsible for lowering the microhardness in both the hardfacings. The variations in the microhardness of hardfacing at different distances from the interface are mainly due to the presence of various phases in the hardfacings. It is observed that the microhardness of NiCrBSi-WC composite hardfacing is significantly higher as compared to NiCrBSi hardfacing which is mainly attributed to the presence of higher volume fraction of hard phases such as WC and W_2C along with chromium carbides and chromium borides as confirmed from the XRD analysis. The improvement in microhardness of NiCrBSi-WC composite hardfacing as compared to NiCrBSi hardfacing is also due to the growth of carbides near the WC reinforcing particles and lower dissolution of WC reinforcing particles. Higher microhardness in case of NiCrBSi-WC hardfacing is beneficial for improvement in slurry abrasive wear resistance. Moreover, the reduction in the thickness of the hardfacing layer can be possible depending upon the service application which can consequently contribute to the reduction in production cost.

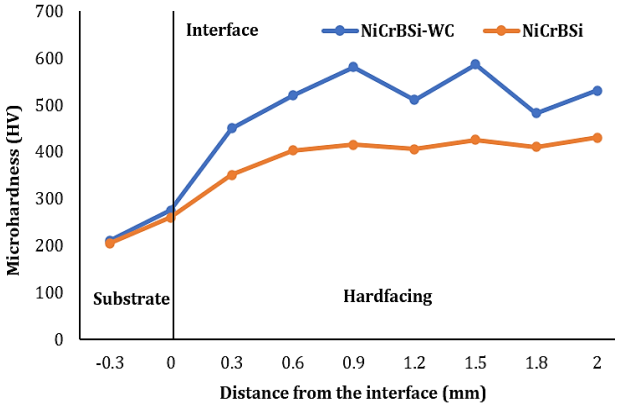

Fig. 10. Microhardness profiles across the interface for NiCrBSi and NiCrBSi-WC samples.

3.3 Slurry abrasive wear analysis

Fig. 11 presents the results of slurry abrasive wear test reported in terms of weight loss of NiCrBSi, NiCrBSi-WC and substrate material as per ASTM G105. The slurry abrasive wear test is conducted twice for each specimen and the average weight loss is considered for comparative analysis. The substrate material 304 ASS showed highest wear loss of 0.087 grams, NiCrBSi hardfacing showed wear loss of 0.005 grams while NiCrBSi-WC showed wear loss of 0.002 grams. The wear resistance of NiCrBSi-WC composite hardfacing is 2.5 times higher than that of NiCrBSi hardfacing and forty times than that of 304 ASS substrate material. It is observed that the wear loss obtained for hardfaced specimens with addition of WC reinforcing particles in NiCrBSi shows lower wear loss as compared to without addition of WC reinforcing particles in NiCrBSi. The minimum wear loss for NiCrBSi-WC composite hardfacing is mainly attributed to higher microhardness due to presence of hard WC and W_2C phases in addition to chromium borides and chromium carbides which act as a highly wear resistant layer. The improvement in slurry abrasive wear resistance of NiCrBSi-WC composite hardfacing as compared to NiCrBSi hardfacing is mainly due to the fact that the applied load is transferred from the soft matrix to the hard WC reinforcing phases which can sustain higher stresses and showed higher wear resistance. The lower dissolution of WC reinforcing particles is also the reason of higher wear resistance of NiCrBSi-WC composite hardfacing.

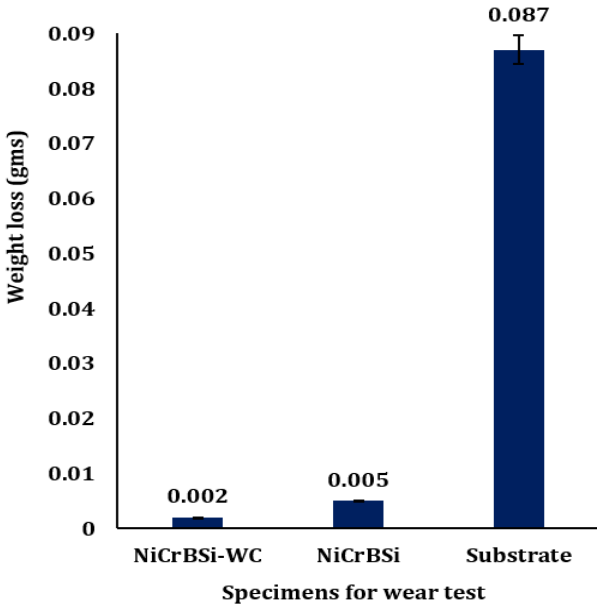

Fig. 11. Slurry abrasive wear performance.

Fig. 12 presents worn-out morphology of NiCrBSi-WC, NiCrBSi hardfacings and substrate material tested as per ASTM G105 in order to understand the dominant wear mechanism. From the analysis, it is observed that parallel grooves are formed on the surface of worn-out speimens resulting from ploughing action caused due to sliding of quartz abrasive sand between the specimen surface and the rubber wheel. The nature of the grooves depends upon the surface hardness of the specimen. As compared to NiCrBSi hardfacing, the worn-out morphology of NiCrBSi-WC showed relatively shallower grooves resulted due to ploughing action along with microcutting and abrasion as wear mechanisms. NiCrBSi hardfacing showed slightly deeper grooves due to ploughing with abrasion and microcutting as wear mechanisms. The substrate material shows the highest wear loss due to presence of wider and deeper grooves caused due to ploughing action along with abrasion, microcutting and plastic deformation as primary wear mechanisms mainly caused due to its comparatively lower hardness.

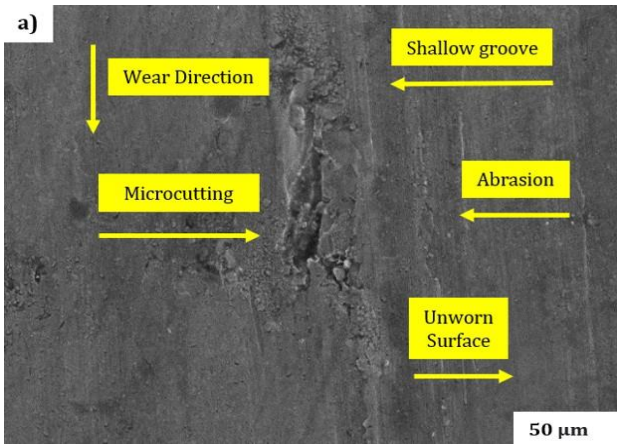

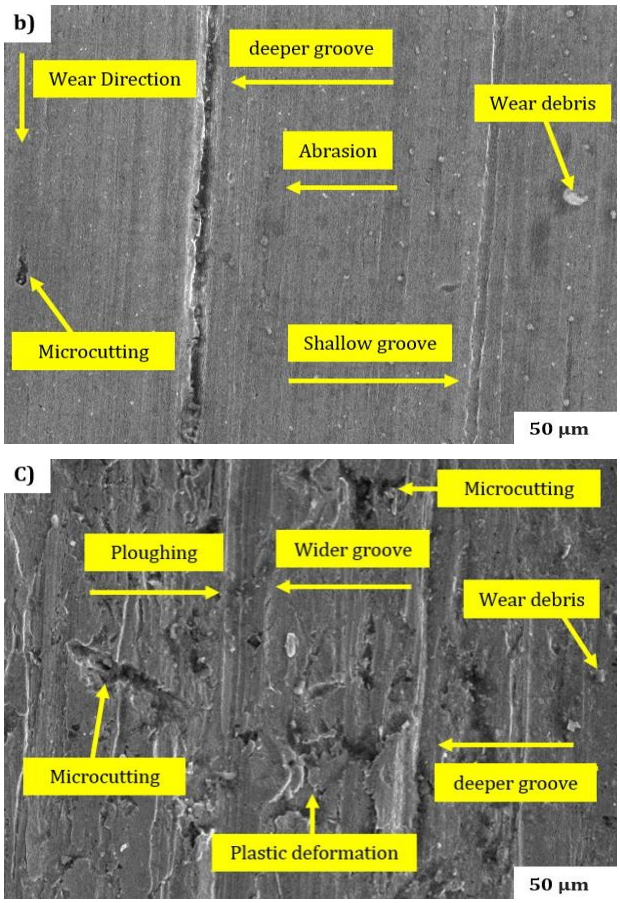

Fig. 12. Worn-out morphology obtained by FESEM as per ASTM G105 for a) NiCrBSi-WC b) NiCrBSi and c) substrate specimens.

3.4 Summary of comparative analysis for NiCrBSi and NiCrBSi-WC hardfacings

The summary of comparative investigations in terms of mechanical and microstructural characterizations for NiCrBSi and NiCrBSi-WC hardfacings is presented in Table 5.

Table 5. Summary of comparative analysis for NiCrBSi and NiCrBSi-WC hardfacing samples.

Sr.No	Basis of comparison	NiCrBSi hardfacing	NiCrBSi-WC hardfacing	Remarks
1	Metallurgical bond	Good	Good	Both hardfacings are suitable.
2	Micro-hardness analysis	Average 405 HV	Average 522 HV	NiCrBSi-WC is suitable.
3	Slurry abrasive wear weight loss	0.005 grams	0.002 grams	NiCrBSi-WC is suitable.
4	Fe % substrate dilution	28.66 %	24.54 %	NiCrBSi-WC hardfacing is suitable.
5	Phases present	γ-Ni, Cr23C6, Cr7C3, CrB, Ni3B, FeNi3 and Fe2Si	γ-Ni, Cr23C6, Cr7C3, CrB, Ni3B, FeNi3, Fe2Si, WC and W2C	NiCrBSi-WC hardfacing is suitable.
6	Micro-structural analysis by FESEM	Interdendritic eutectic precipitations, needle shaped precipitates and nickel solid solution.	WC reinforcing particles are well dispersed in the nickel matrix along with needle shaped precipitates.	NiCrBSi-WC hardfacing is suitable.
7	Worn-out morphology	Comparatively deeper grooves resulted due to ploughing action along with microcutting and abrasion.	Comparatively shallower grooves are formed due to ploughing action along with microcutting and abrasion.	NiCrBSi-WC hardfacing is suitable.

The comparative analysis revealed that the NiCrBSi-WC composite hardfacing is advantageous as compared to NiCrBSi hardfacing almost in all aspects. Considering the higher microhardness and higher wear resistance of NiCrBSi-WC hardfacing, the thickness of the hardfacing can be reduced as per the service applicability which may contribute to the reduction in the production cost in addition to the enhanced service life.

4. CONCLUSIONS

From the multi-track experiments performed by PTAW on 304 ASS with NiCrBSi and NiCrBSi-WC composite hardfacings, following conclusions are drawn:

1. The crack-free deposition of NiCrBSi hardfacing with and without addition of WC reinforcing particles is achieved with the proposed PTAW process parameters.
2. The NiCrBSi-WC composite hardfacing and NiCrBSi hardfacing shows good metallurgical bond with AISI 304 ASS substrate material as revealed from microstructural analysis.
3. The typical microstructure of the NiCrBSi hardfacing consists of γ-Ni, $Cr_{23}C_6$, Cr_7C_3, CrB, Fe_2Si, $FeNi_3$ and Ni_3B phases and the NiCrBSi-WC hardfacing consists of WC and W_2C phases along with γ-Ni, $Cr_{23}C_6$, Cr_7C_3, CrB, Fe_2Si, $FeNi_3$ and Ni_3B.
4. The wear resistance of NiCrBSi-WC composite hardfacing is significantly higher which is 2.5 times that of NiCrBSi hardfacing and forty times than that of substrate material which is mainly attributed to the presence of WC and W_2C hard ceramic phases along with chromium carbides and chromium borides phases.
5. The worn-out morphology of NiCrBSi-WC hardfacing shows comparatively shallower grooves along with microcutting and abrasion which resulted in lower mass loss as compared to NiCrBSi hardfacing. The substrate material showed wider and deeper grooves resulted due to ploughing action along with abrasion, microcutting and plastic deformation as primary wear mechanisms of material removal.

Considering the significant improvement in slurry abrasive wear resistance with addition of WC reinforcing particles in NiCrBSi hardfacing, the NiCrBSi-WC hardfacing is recommended which may be beneficial to enhance service-life of slurry pipelines used in mineral processing industries.

Acknowledgement

The authors thankfully acknowledge the financial support provided by The Institution of Engineers (India) for carrying out research and development work in this subject.

REFERENCES

[1] A. Rathod, S. Sapate, R. Khatirkar, *Effect of composition and microstructure on slurry abrasion response of hardfaced martensitic stainless steel*, Tribology-Materials, Surfaces & Interfaces, vol. 10, iss. 1, pp. 45-52, 2016, doi: 10.1080/17515831.2015.1126907

[2] Y. Xie, J.J. Jiang, K.Y. Tufa, S. Yick, *Wear resistance of materials used for slurry transport*, Wear, vol. 332, pp. 1104-1110, 2015, doi: 10.1016/j.wear.2015.01.005

[3] J. Singh, S. Kumar, S.K. Mohapatra, *Erosion Wear Performance of Ni-Cr-O and NiCrBSiFe-WC (Co) Composite Coatings Deposited by HVOF Technique*, Industrial Lubrication and Tribology, vol. 71, no. 4, pp. 610-619, 2019, doi: 10.1108/ILT-04-2018-0149

[4] K. Holmberg, P. Kivikyto-Reponen, P. Harkisaari, K. Valtonen, A. Erdemir, *Global energy consumption due to friction and wear in the mining industry*, Tribology International, vol. 115, pp. 116-139, 2017, doi: 10.1016/j.triboint.2017.05.010

[5] J.M.S. De Sousa, F. Ratusznei, M. Pereira, R. De Medeiros Castro, E.I.M. Curi, *Abrasion resistance of Ni-Cr-B-Si coating deposited by laser cladding process*, Tribology International, vol. 143, pp. 1-11, 2020, doi: 10.1016/j.triboint.2019.106002

[6] M. Petrica, C. Katsich, E. Badisch, F. Kremsner, *Study of abrasive wear phenomena in dry and slurry 3-body conditions*, Tribology International, vol. 64, pp. 196-203, 2013, doi: 10.1016/j.triboint.2013.03.028

[7] C.S. Ramachandran, V. Balasubramanian, R. Varahamoorthy, S. Babu, *effect of slurry concentration, abrasive particle size and velocity on wear behaviour of nickel based (colmonoy) plasma*

transferred arc hardfaced surface, surface, Engineering, vol. 25, iss. 6, pp. 449-457, 2009, doi: 10.1179/174329408X309938

[8] S.G. Sapate, A.D. Chopde, P.M. Nimbalkar, D.K. Chandrakar, *Effect of microstructure on slurry abrasion response of En-31 steel,* Materials & Design, vol. 29, iss. 3, pp. 613-621, 2008, doi: 10.1016/j.matdes.2007.02.014

[9] V. Balasubramanian, R. Varahamoorthy, C.S. Ramachandran, S. Babu, *Abrasive slurry wear behavior of stainless steel surface produced by plasma transferred arc hardfacing process*, Surface and Coatings Technology, vol. 202, iss. 16, pp. 3903-3912, 2008, doi: 10.1016/j.surfcoat.2008.01.031

[10] S.R. More, D.V. Bhatt, J.V. Menghani, *Study of The Parametric Performance of Solid Particle Erosion Wear Under the Slurry Pot Test Rig*, Tribology in Industry, vol. 39, no. 4, pp. 471-481, 2017, doi: 10.24874/ti.2017.39.04.06

[11] A.P. Thummar, S.P. Wanare, V.D. Kalyankar, *Effect of Dilution on Microstructure and Slurry Abrasive Wear Behaviour of Ni-Cr-Mo-W Coating on 304 Stainless Steel Deposited by Synergic Pulsed Gas Metal Arc Welding*, Tribology in Industry, vol. 39, no. 4, 2021, doi: 10.24874/ti.984.10.20.01

[12] P. Wang, Y. Zhang, D. Yu, *Microstructure and Mechanical Properties of Pressure-Quenched SS304 Stainless Steel*, Materials, vol. 12, iss. 2, pp. 1-9, 2019, doi: 10.3390/ma12020290

[13] C. Guoqing, F. Xuesong, W. Yanhui, L. Shan, Z. Wenlong, Microstructure and Wear Properties of Nickel-Based Surfacing Deposited by Plasma Transferred Arc Welding, Surface and Coatings Technology, vol. 228, pp. S276-S282, 2013, doi: 10.1016/j.surfcoat.2012.05.125

[14] T. Liyanage, G. Fisher, A.P. Gerlich, *Microstructures and abrasive wear performance of PTAW deposited Ni–WC overlays using different ni-alloy chemistries*, Wear, vol. 274, pp. 345-354, 2012, doi: 10.1016/j.wear.2011.10.001

[15] V.D. Kalyankar, H.V. Naik, S. Shah, *Metallographic Characterization and Comparative Analysis of SS-309L and Inconel 625 As Buffer Layer Materials on P91 Steel*, Practical Metallography, vol. 57, no. 12, pp. 828-852, 2020, doi: 10.3139/147.110667

[16] M. Benegra, G. Pintaude, A.S.C.M. D'Oliveira, H. *Goldenstein, Characterization of NiCrAlC PTA Coatings, Materials Research*, vol. 15, no. 5, pp. 775-778, 2012, doi: 10.1590/S1516-14392012005000098

[17] Z. Cai, Y. Wang, X. Cui, G. Jin, Y. Li, Z. Liu, M. Dong, *Design and microstructure characterization of FeCoNiAlCu high-entropy alloy coating by plasma cladding: in comparison with thermodynamic calculation*, Surface and Coatings Technology, vol. 330, pp. 163-169, 2017, doi: 10.1016/j.surfcoat.2017.09.083

[18] D.D. Deshmukh, V.D. Kalyankar, *recent status of overlay by plasma transferred arc welding technique,* International Journal of Materials and Product Technology, vol. 56, no. 1-2, pp. 23-83, 2018, doi: 10.1504/IJMPT.2018.089118

[19] D.D. Deshmukh, V.D. Kalyankar, Deposition *Characteristics of Multitrack Overlay by Plasma Transferred Arc Welding on SS316L with Co-Cr Based Alloy – Influence of Process Parameters*, High Temperature Materials and Processes, vol. 38, pp. 248-263, 2019, doi: 10.1515/htmp-2018-0046

[20] A. Maslarevic, G.M. Bakic, M.B. Djukic, B. Rajicic, V. Maksimovic, V. Pavkov, *Microstructure and Wear Behavior of MMC Coatings Deposited by Plasma Transferred Arc Welding and Thermal Flame Spraying Processes*, Transactions of the Indian Institute of Metals, vol. 73, no. 1, pp. 259-271, 2020, doi: 10.1007/s12666-019-01831-9

[21] K. Deenadayalan, V. Murali, *Role of various weight percentages of wc particle on interface thickness and friction-wear property of NiCrBSi-WC composite fabricated using PTAW process,* Materials Research Express, vol. 6, no. 4, 2019, doi: 10.1088/2053-1591/aafd4f

[22] V.D. Kalyankar, H.V. Naik, Overview of metallurgical studies on weld deposited surface by plasma transferred arc technique, Metallurgical Research & Technology, vol. 118, no. 1, 2021, doi: 10.1051/metal/2020088

[23] A. Gatto, E. Bassoli, M. Fornari, *Plasma Transferred Arc deposition of powdered high performances alloys: process parameters optimisation as a function of alloy and geometrical configuration*, Surface and Coatings Technology, vol. 187, iss. 2-3, pp. 265-271, 2004, doi: 10.1016/j.surfcoat.2004.02.013

[24] K. Gurumoorthy, M. Kamaraj, K.P. Rao, A.S. Rao, S. Venugopal, *Microstructural aspects of plasma transferred arc surfaced ni-based hardfacing alloy*, Materials Science and Engineering: A, vol. 456, iss. 1-2, pp. 11-19 ,2007, doi.org/10.1016/j.msea.2006.12.121

[25] C. Sudha, P. Shankar, R.S. Rao, R. Thirumurugesan, M. Vijayalakshmi, B. Raj, *Microchemical and microstructural studies in a PTA weld overlay of Ni–Cr–Si–B alloy on AISI 304L stainless steel*, Surface and Coatings Technology, vol. 202, iss. 10, pp. 2103-2112, 2008, doi: 10.1016/j.surfcoat.2007.08.063

[26] S. Oukach, B. Pateyron, L. Pawłowski, *Physical and chemical phenomena occurring between solid ceramics and liquid metals and alloys at laser and plasma composite coatings formation: A review*, Surface Science Reports, vol. 74, iss. 3, pp. 213-241, 2019, doi: 10.1016/j.surfrep.2019.06.001

[27] X. Guozhi, S. Xiaolong, Z. Dongjie, W. Yuping, L. Pinghua, *Microstructure and corrosion properties of thick WC composite coating formed by plasma cladding*, Applied Surface Science, vol. 256, iss. 21, pp. 6354-6358, 2010, doi: 10.1016/j.apsusc.2010.04.016

[28] C. Just, E. Badisch, J. Wosik, *Influence of welding current on carbide/matrix interface properties in MMCs*, Journal of Materials Processing Technology, vol. 210, iss. 2, pp. 408-414, 2010, doi: 10.1016/j.jmatprotec.2009.10.001

[29] R. L. Deuis, J.M. Yellup, C. Subramanian, *Metal-matrix composite coatings by pta surfacing*, Composites Science and Technology, vol. 58, iss. 2, pp. 299-309, 1998, doi: 10.1016/S0266-3538(97)00131-0

[30] R. Sundaramoorthy, S.X. Tong, D. Parekh, C. Subramanian, *Effect of matrix chemistry and WC types on the performance of Ni-WC based MMC overlays deposited by plasma transferred arc (PTA) welding*, Wear, vol. 376, pp. 1720-1727, 2017, doi: 10.1016/j.wear.2017.01.027

[31] J. Nurminen, J. Nakki, P. Vuoristo, *Microstructure and properties of hard and wear resistant MMC coatings deposited by laser cladding*, International Journal of Refractory Metals and Hard Materials, vol. 27, iss. 2, pp. 472-478, 2009, doi: 10.1016/j.ijrmhm.2008.10.008

[32] V. Ramasubbu, G. Chakraborty, S.K. Albert, A.K. Bhaduri, *Effect of dilution on GTAW Colmonoy 6 (AWS NiCr–C) hardface deposit made on 316LN stainless steel*, Materials Science and Technology, vol. 27, iss. 2, pp. 573-580, 2011, doi: 10.1179/026708309X12526555493431

[33] F. Fernandes, B. Lopes, A. Cavaleiro, A. Ramalho, A. Loureiro, *Effect of arc current on microstructure and wear characteristics of a Ni-based coating deposited by PTA on gray cast iron*, Surface and Coatings Technology, vol. 205, no. 16, pp. 4094-4106, 2011, doi: 10.1016/j.surfcoat.2011.03.008

[34] V.D. Kalyankar, H.V. Naik, *Influence of Welding Position on Tribological Behavior of SS-309L Cladded Surface on 9Cr-1Mo Steel*, Tribology in Industry, vol. 43, no. 2, 2020, doi: 10.24874/ti.906.06.20.11

[35] L. Zunake, V.D. Kalyankar, *On the performance of weld overlay characteristics of Ni–Cr–Si–B deposition on 304 ASS using synergetic pulse-GMAW Process*, Science and Technology of Welding and Joining, vol. 26, iss. 2, pp. 106-115, 2021, doi: 10.1080/13621718.2020.1846935

[36] H. Zhang, Y. Shi, M. Kutsuna, G.J. Xu, *Laser cladding of colmonoy 6 powder on AISI316L austenitic stainless steel*, Nuclear Engineering and Design, vol. 240, iss. 10, pp. 2691-2696, 2010, doi: 10.1016/j.nucengdes.2010.05.040

[37] Z. Weng, A. Wang, X. Wu, Y. Wang, Z. Yang, Wear *Resistance of diode laser-clad Ni/WC composite coatings at different temperatures*, Surface and Coatings Technology, vol. 304, pp. 283-292, 2016, doi: 10.1016/j.surfcoat.2016.06.081

[38] ASTM G105-16, Standard Test Method for Conducting Wet Sand/rubber Wheel Abrasion Tests, 2016.

[39] C. Guo, J. Zhou, J. Chen, J. Zhao, Y. Yu, H. Zhou, *High temperature wear resistance of laser cladding NiCrBSi and NiCrBSi/WC-Ni composite coatings*, Wear, vol. 270, iss. 7-8, pp. 492-498, 2011, doi: 10.1016/j.wear.2011.01.003

[40] I. Hemmati, V. Ocelik, K. Csach, J.T.M. De Hosson, *Microstructure and Phase Formation in A Rapidly Solidified Laser-Deposited Ni-Cr-B-Si-C Hardfacing Alloy*, Metallurgical and Materials Transactions A, vol. 45, iss. 2, pp. 878-892, 2014, doi: 10.1007/s11661-013-2004-4

[41] L. Da Silva, A. D'Oliveira, *NiCrSiBC coatings: effect of dilution on microstructure and high temperature tribological behaviour*, Wear, vol. 350, pp. 130-140, 2016, doi: 10.1016/j.wear.2016.01.015

[42] X. Men, F. Tao, L. Gan, F. Zhao, *Erosion behavior of Ni-based coating under high-speed hot airflow*, Surface Engineering, vol. 35, iss. 8, pp. 710-718, 2019, doi: 10.1080/02670844.2019.1573343